

## Numerical Study of a Moving Object in Calm Water Using Overset and Non-overset Grids

Yao Peng<sup>1,2</sup>, Decheng Wan<sup>1,2\*</sup>, Gang Chen<sup>1,2</sup>, Wenhua Huang<sup>3</sup>

1 State Key Laboratory of Ocean Engineering, School of Naval Architecture, Ocean and Civil Engineering, Shanghai Jiao Tong University,

2 Collaborative Innovation Center for Advanced Ship and Deep-Sea Exploration, Shanghai, China

3 School of Science, Huzhou University, Huzhou, China

\*Corresponding author

### ABSTRACT

In this paper, a numerical solver for naval architecture and ocean engineering named naoe-FOAM-SJTU solver, which is developed using OpenFOAM, is applied to conduct the simulation of a special object moving in calm water. The main part of the object goes forward under the free surface of water, whereas a slender rod of the object stretches out of the water. To better simulate the situation, this research use two different grids. One is the traditional non-overset grids, and the other is overset grids. Results of both grids are compared in regard of forces, wave patterns and velocities. The object moves at two different speeds (5kn and 6kn), while the moving direction, which is named as x-direction, is always parallel to the free surface of water. The similarities and differences of the result calculated out by the two grids are discussed. This paper also discusses the influence of moving speed on the wave pattern, resistance and velocity field.

KEY WORDS: naoe-FOAM-SJTU solver; calm water resistance; wave-pattern; overset grid.

### INTRODUCTION

The prototype of the research object is a special kind of ship. And the designers want to see the dynamic performance of this model through numerical simulation. The main purpose of this paper is to find out the characteristics of the wave pattern, resistance and velocity field when the special object moves at a constant velocity in calm water. The research object can be divided into two parts. The main part of the object goes forward under the free surface of water, whereas a slender rod of the object stretching out of the water.

Both overset and non-overset grids are used to better simulate the situation. This paper focus on the influence of different moving speed on the result. And this paper also pay attention to the comparison of results calculated out by different types of grids.

### THEORIES

The present solver naoe-FOAM-SJTU adopted for numerical simulation is based on a built-in solver in OpenFOAM named

interDyMFoam, which can be used to solve two incompressible, isothermal immiscible fluids with dynamic mesh motion. People can use this solver to deal with calm-water resistance problem basing on traditional non-overset grid. And our experiences reflect that it is difficult for us to deal with the situation in which the different part of research object has relative movement. So a solver named naoeFoam-os-SJTU is developed by Prof. Decheng Wan's group to better simulate multi-component objects by using overset grids. This paper uses both naoe-FOAM-SJTU and naoeFoam-os-SJTU to conduct the numerical simulation. Mathematical formulae and recapitulative theories related to the two solvers are described as follows in detail.

### Governing Equations

For transient, incompressible and viscous fluid, flow problems are governed by Navier-Stokes equations:

$$\nabla \cdot \mathbf{U} = 0 \quad (1)$$

$$\frac{\partial \rho \mathbf{U}}{\partial t} + \nabla \cdot (\rho (\mathbf{U} - \mathbf{U}_g) \mathbf{U}) = -\nabla p_d - \mathbf{g} \cdot \mathbf{x} \nabla \rho + \nabla \cdot (\mu_{eff} \nabla \mathbf{U}) + (\nabla \mathbf{U}) \cdot \nabla \mu_{eff} + \mathbf{f}_\sigma + \mathbf{f}_s \quad (2)$$

where  $\mathbf{U}$  and  $\mathbf{U}_g$  represent velocity of flow field and grid nodes

separately;  $p_d = p - \rho \mathbf{g} \cdot \mathbf{x}$  is dynamic pressure of flow field by subtracting the hydrostatic part from total pressure  $p$ ;  $\mathbf{g}$  denotes the gravity acceleration vector;  $\rho$  represents density;  $\mu_{eff}$  represents effective viscosity coefficient, and  $\mu_{eff} = \rho(\nu + \nu_t)$ , where  $\nu$  is the coefficient of kinematic viscosity,  $\nu_t$  is the coefficient of eddy viscosity,  $\nu_t$  is obtained from  $k-\omega$  turbulence model;  $\mathbf{f}_\sigma$  is surface tension which only takes effect at the free surface and equals zero elsewhere.

### Free Surface Capturing

Volume of Fluid (VOF) method is adopted in OpenFOAM to capture free surface. In this method, Volume fraction function denoted as  $\alpha$  is defined for every cell, representing the ratio of cell volume where the

fluid occupies. The physical meaning of  $\alpha$  is defined as Eq. 3:

$$\begin{cases} \alpha = 0, & \text{air} \\ \alpha = 1, & \text{water} \\ 0 < \alpha < 1, & \text{free surface} \end{cases} \quad (3)$$

The volume fraction function  $\alpha$  is governed by Eq. 4:

$$\frac{\partial \alpha}{\partial t} + \nabla \cdot [(\mathbf{U} - \mathbf{U}_g)\alpha] + \nabla \cdot [\mathbf{U}_r(1 - \alpha)\alpha] = 0 \quad (4)$$

To better capture free surface, a bounded compression technique (Rusche, 2002) is adopted which introduces an additional compression term on the left-hand side of Eq. 4, where  $\mathbf{U}_r$  is a relative velocity field. The compression term only functions near free surface due to  $(1 - \alpha)\alpha$ . During the procedure, Eq. 4 is solved to obtain volume fraction of each cell and free surface is then determined.

For two-phase flow problems, the physical properties of one fluid are calculated as weighted averages based on volume fraction of water and gas in one cell as Eq. 5:

$$\begin{cases} \rho = \alpha\rho_l + (1 - \alpha)\rho_g \\ \mu = \alpha\mu_l + (1 - \alpha)\mu_g \end{cases} \quad (5)$$

Where subscripts  $l$  and  $g$  denote liquid and gas separately.

### Overset Grid Theory

The so-called overset method is to generate grid for each component of the simulating object separately, and then enclose these grids in a background grid. After the procedures of digging holes and modifying meshes, the meshes outside of computational domain or inside of the object are removed. And the data in the mesh-overlap areas is interpolated. Meanwhile, information exchanges through the mesh-overlap area from one mesh to another.

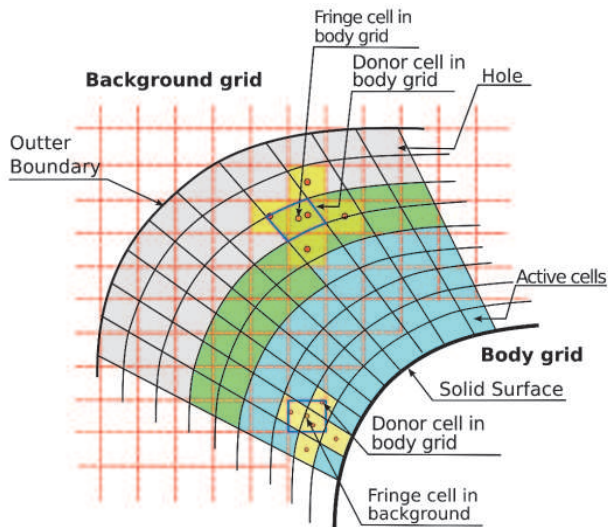


Fig.1 Sketch of overset grid

Fig.1 contains two sets of grids, which are named as body grid

and background grid. Fig.1 also shows the basic elements of overset grids. In naoeFoam-os, information is contained in the center of every cell, which is called Cell-Centered. Obviously, there are 5 kinds of cells shown in Fig.1, such as active cell, hole, fringe cell, donor cell and orphan. They play different roles in the calculation of naoeFoam-os-SJTU (Shen and Wan, 2015).

The active cell has the same function of normal cells in non-overset grid. It participates in calculation and contains real information of flow field. The hole is the cell which is outside of computational domains or inside the object. It will be removed out of calculation. The fringe cell gets information from other cells. It occurs in the mesh-overlap areas and is located between holes and active cells. The donor cell offers information to the interpolating-area. The orphan is a special kind of cell. When a cell in interpolating-area can not find a donor cell nearby, it will be regarded as an orphan.

The interpolation of the overset grid depends on the calculation of DCI. And naoeFoam-os use SUGGAR (Ralph Noack, 2005) to generate DCI. To know more details of the procedure, you can refer to manual of naoeFoam-os-SJTU (Shen and Wan, 2015).

### COMPUTATIONAL MODEL

An object with a special appearance is selected in this study. The prototype of the model is confidential, so I simplified the model in this paper in order not to make trouble. Readers can simply regard the model as a small submarine with a periscope.

### Model Parameters

The main part of the model goes forward under the free surface of water, whereas a slender rod of the model stretching out of the water. The appearance is shown in Fig.2, and the rod of the model inclines 15 degree compare to vertical direction when the model is moving. The parameters of this model are listed in Table 1.



(a) Side view

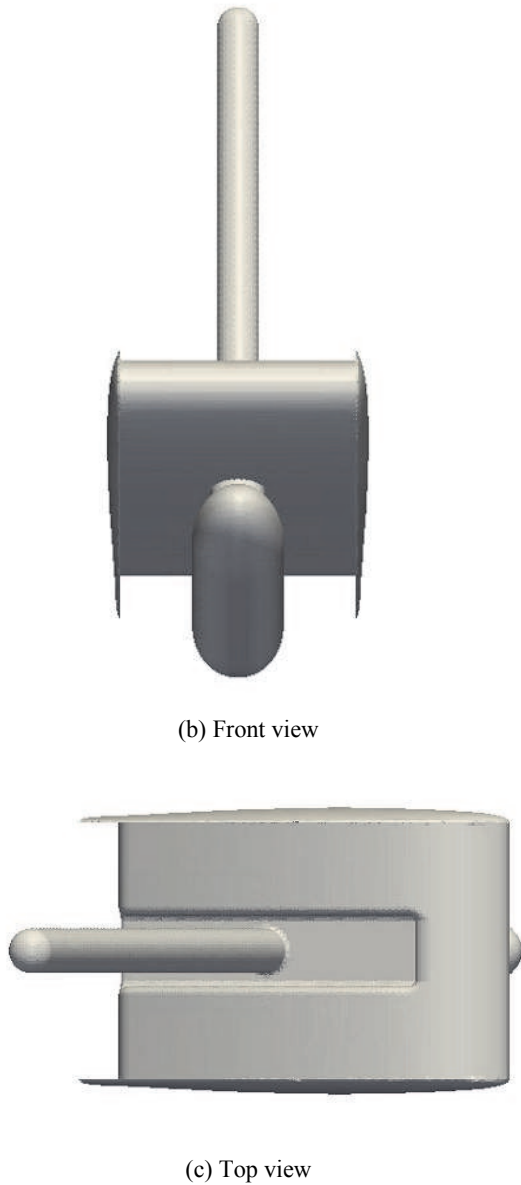


Fig.2 Sketch of the model

### Computational Domains

This paper uses two sets of grids, one is overset grid, and the other is non-overset grid. OpenFOAM provides users with a very powerful utility called snappyHexMesh to help create computational mesh with high quality. Fig.3 shows the non-overset grid. As seen from the figure, a rectangular numerical tank is used with its dimensions as  $L[-16m, 4m] \times W[-8m, 8m] \times H[-10m, 10m]$ . The computational model is located at the origin  $(0, 0, 0)$ . Since the fluid field near free surface and the model varies rather violently, meshes are densified in these regions. A sponge area with the length of 4m is set at the back of x-direction.

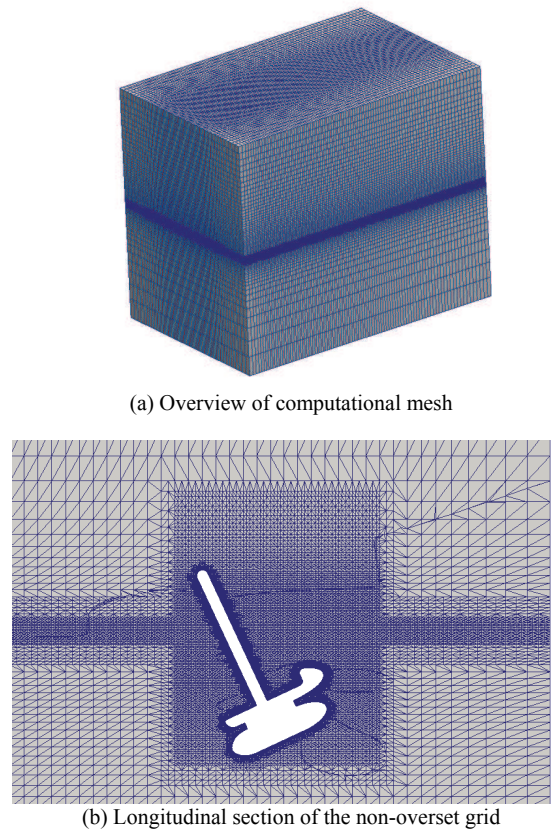
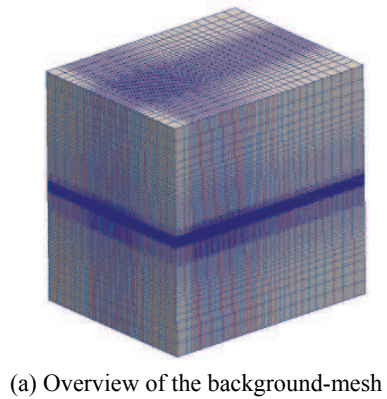
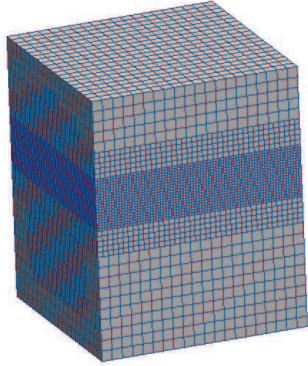


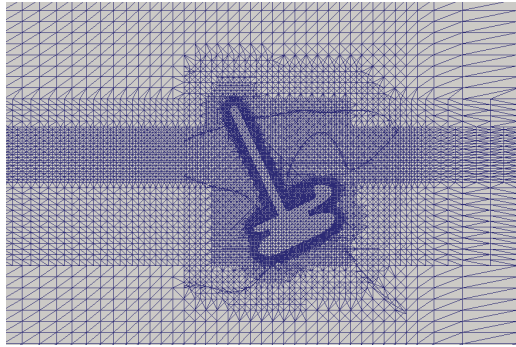
Fig.3 Global and local view of computational mesh (non-overset grid)

Fig.4 shows the overset grid which consists of 2 parts, background grid and hull grid. As seen from the figure, the background grid is a rectangular block with its dimensions as  $L[-12m, 4m] \times W[-8m, 8m] \times H[-10m, 10m]$ . And the hull grid is a rectangular block with its dimensions as  $L[-2m, 2m] \times W[-2m, 2m] \times H[-3m, 2m]$ . The computational model is also located at the origin  $(0, 0, 0)$ . And meshes near water surface and the model are refined. It must be pointed out that the background grid is smaller than the non-overset grid because there is not a sponge area.





(b) Overview of the hull-mesh



(c) Longitudinal section of the overset grid

Fig.4 Global and local view of computational mesh (overset grid)

## NUMERICAL RESULTS

This paper chooses 3 typical numerical results to discuss, which are listed in Table 2. Comparison of result A and B shows the influence of moving speed and comparison of result B and C shows the similarities and differences of using overset and non-overset grid.

Table 2. Simulating conditions

NO.	Grid	Speed
Result A	non-overset grid	5kn (2.572m/s)
Result B	non-overset grid	6kn (3.086m/s)
Result C	overset grid	6kn (3.086m/s)

### Typical Result

The prototype of this model moves in a speed of 6kn in normal condition, so this paper choose Result B as a typical result to discuss. In fact, when we conduct the simulation of the model by using non-overset grid, we adopt the concept relative velocity. In this condition, we regard the situation A equalize to the situation B, so we fix the location of model and generate a uniform flow with a constant speed 6kn. Situation A and B are defined in Table 3. However, when we conduct the numerical simulation by using overset grid, we let the model move forward at a constant speed in calm water.

Table 3. Two situations about the relative speed.

Items	Value
Situation A	Model moves at a constant speed in calm water
Situation B	Model is fixed, and here comes a uniform flow with a constant speed

Fig.5 shows the result when the wave pattern induced by the model becomes stable. Model moves from left to right. And waves spread from the waterline plane of the model towards backward and both sides. It can be seen from the figure that the main wave patterns induced by the model are transverse waves, and this result is identical with the fact the main wave patterns induced by submarines are transverse waves. The highest peak of wave crest, near 0.3m, occurs in the first wave crest after the model, and the lowest nadir of wave trough, near -0.3m, occurs in the first wave trough around the model.

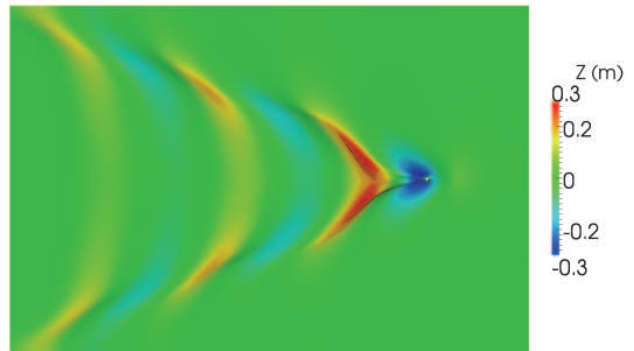


Fig.5 Wave pattern at the speed of 6 kn (non-overset grid)

Fig.6 shows the velocity of the free-surface particles in x-direction, which is the model-moving direction. It is important to point out that, as previously stated, we make the model fixed and generate a uniform and constant flow to simulate the moving speed. So the value in Fig.6 just shows the relative velocity of water particles compared to the model. As seen from the figure, the velocity of water particles become bigger, compared to the initial velocity -3.086m/s, near wave crest. And the velocity of water particles become smaller near wave trough.

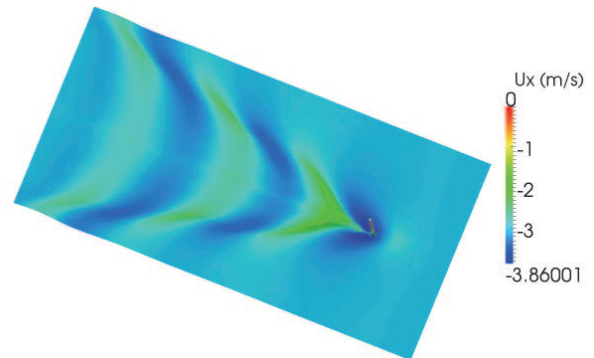


Fig.6 Relative velocity in x-direction of the free-surface particles

Fig.7 shows the longitudinal section of the wave pattern and model. As seen from the figure, the first wave pattern occurs after the model is wave trough, and it is followed by a wave crest. And we can find that the amplitude of wave becomes smaller as the distance to the model becomes larger.

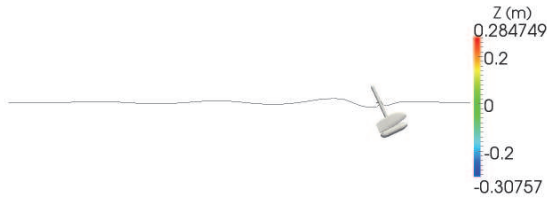


Fig.7 Longitudinal section of wave pattern and model

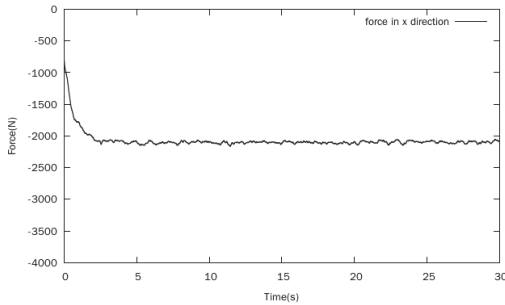
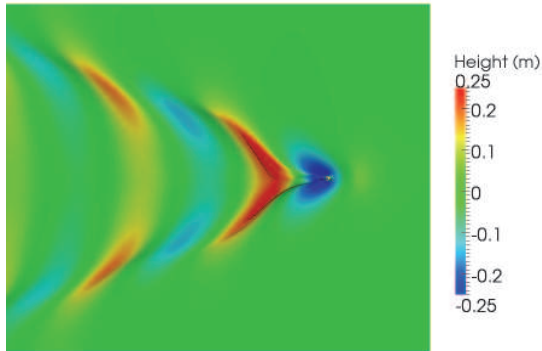
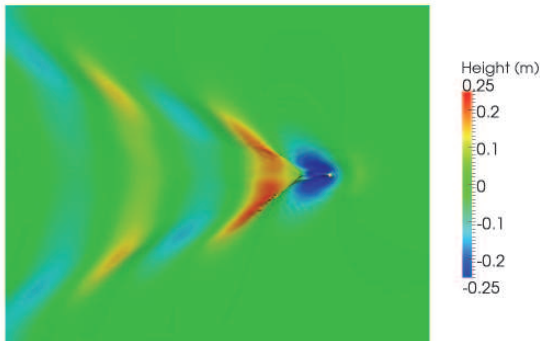


Fig.8 Resistance of the model in x-direction



(a) Wave pattern at 6kn (non-overset grid)



(b) Wave pattern at 6kn (overset grid)

Fig.9 Wave pattern at the speed of 6kn

Fig.8 shows the force the object suffers when it moves in x-direction. We can find in Fig.8 that the resistance of the model tends to reach a stable value which is close to 2100N.

### Comparison of the Result of Using Overset Grid and Non-overset Grid

This study simulates the model by using both overset grid and non-overset grid, and it seems necessary to make a comparison about the result of these two grids. The most obvious difference occurs in the procedure of doing the post-processing. As previously mentioned, the model remains immobilized while a uniform and constant flow comes from the inlet boundary in the non-overset grid, and as a contrast the model moves forward with the whole computational domain at a constant speed in calm water in the overset grid.

Fig.9 shows the results of wave patterns of these two grids when the calculation becomes stable. The model moves at 6kn in this simulation. As seen from the figure, the wave patterns look very similar, and the wave crest and wave trough occurs in the same area however the value appears a little difference. This difference may be induced by numerical fault or the different grid-precision in some places. Therefore, it is worthful for our future work to learn more about the cause and to minimize the difference.

Fig.10 shows the result of the resistance in x-direction using different grids. As seen from the figure, no matter use overset grid or non-overset grid, the result tends to reach 2100N.

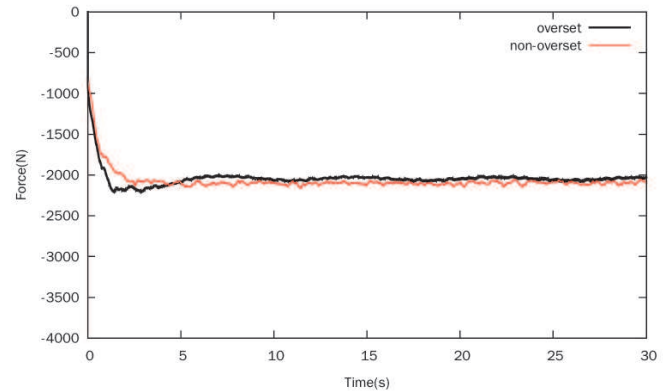
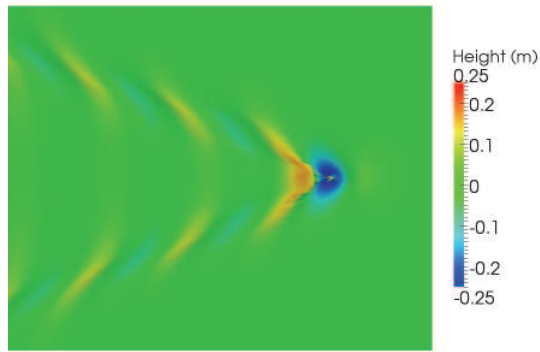


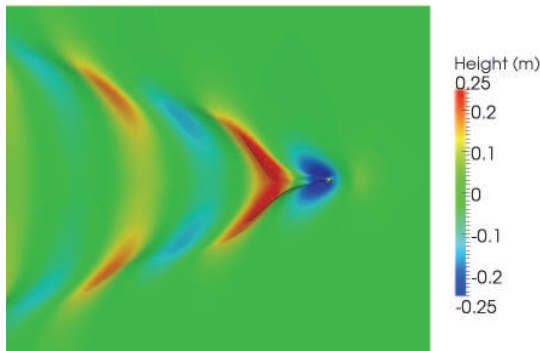
Fig.10 Comparison of the resistance calculated by overset grid and non-overset grid

### Comparison of the Results When the Object Moves at 5kn and 6kn

This chapter compares the results when the object moves in the calm water at the speed of 5kn and 6kn by using non-overset grid. Fig.11 shows the wave patterns induced by the object at different moving speed. We can see it clearly that the wave amplitude is bigger when the model moves faster. Also, the faster the model moves, the bigger the distance between the adjacent wave crest is. The highest peak of wave crest occurs in the first wave crest after the model, and the lowest nadir of wave trough occurs in the first wave trough around the model.



(a) Wave pattern at 5kn



(b) Wave pattern at 6kn

Fig.11 Wave pattern at different moving speed

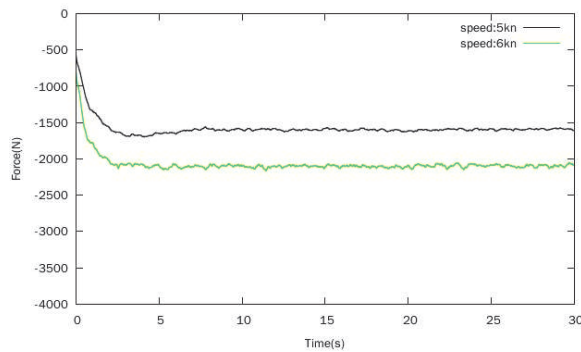
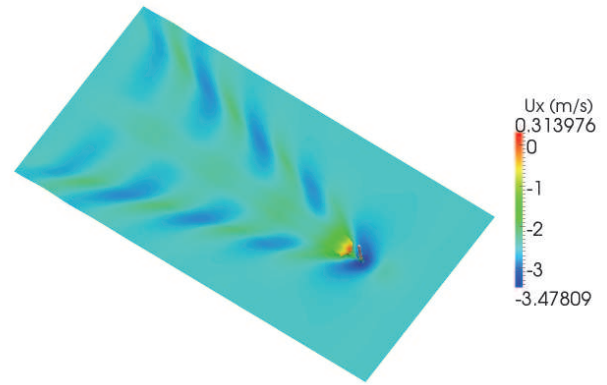


Fig.12 Resistance of the model at different moving speed

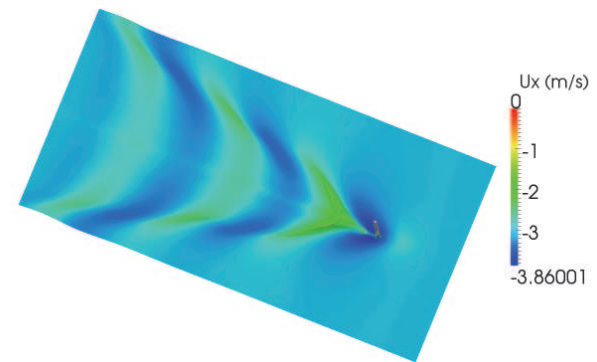
Fig.12 shows the result of the resistance in x-direction when the model moves at the speed of 5kn and 6kn in calm water. As seen from the figure, the model suffers larger force when it moves faster in calm water. By the way, a business software is used to simulate the same condition, the result of the total resistance is 1500N whereas my result is 1500N (At the speed of 5kn), and 2300N whereas my result is 2100N (At the speed of 6kn). We can qualitatively make sure that our results are right.

Fig.13 shows the velocity of the free surface particles in x-direction. It

is important to point out that, as previously stated, we make the model fixed and generate a uniform and constant flow to simulate the moving speed. So the value in Fig.13 just shows the relative velocity of water particles compared to the model. For each individual water particle, the relative velocity in x-direction has close relationship with the particle's height. Generally, the velocity of water particles become bigger, compared to the initial velocity, near wave crest, and the velocity of water particles become smaller near wave trough.



(a) Relative velocity in x-direction (moving speed: 5kn)



(b) Relative velocity in x-direction (moving speed: 6kn)

Fig.13 Relative velocity in x-direction of the free-surface particles

## CONCLUSIONS

In this study, two viscous flow solvers, which are named as 'naoe-Foam-SJTU' and 'naoe-Foam-os', are adopted to conduct the simulation. Both of these two solvers are developed based on the open source toolbox OpenFOAM. Solver naoeFoam-SJTU requires non-overset grid and solver naoeFoam-os requires overset grid. By comparing numerically calculated results of a same working condition for a special model using different types of grids, we can find the similarities and differences of these two solvers. And by comparing the results of wave patterns and forces at different moving speed, we find out some qualitative rules. Conclusions can be drawn as follows.

- (1) The amplitude of a wave becomes smaller as its longitudinal distance to model becomes larger. The relative velocity of the water particles become larger, compared to the initial velocity, near wave crest. And the velocity of water particles become smaller near wave trough.

(2) The results of wave pattern, water-particle velocity and model resistance calculated out by using non-overset grid and overset grid look similar. The main difference of these two methods occurs in the procedure of post-processing.

(3) The wave amplitude is bigger when the model moves faster. Also, the faster the model moves, the bigger the distance between adjacent wave crest is. Moreover, the resistance of the model is larger when it moves faster.

Although in this study, we only set free one degree of freedom, it can be easily extended to 6 degree-of-freedom motion. And the result in this study shows there are still some differences between using overset grid and non-overset grid. The work done in this paper can serve as the foundation for our future relevant studies such as the simulation of complex floating structures.

#### ACKNOWLEDGEMENTS

This work is supported by the National Natural Science Foundation of China (51379125, 51490675, 11432009, 51579145, 11272120), Chang Jiang Scholars Program (T2014099), Program for Professor of Special Appointment (Eastern Scholar) at Shanghai Institutions of Higher Learning (2013022), Innovative Special Project of Numerical Tank of Ministry of Industry and Information Technology of China (2016-23) and Foundation of State Key Laboratory of Ocean Engineering (GKZD010065), to which the authors are most grateful.

#### REFERENCES

Cao, H., Wan, DC (2014). "Development of Multidirectional Nonlinear Numerical Wave Tank by naoe-FOAM-SJTU Solver," *International Journal of Ocean System Engineering*, 4(1):52-59.

Cao, H., Zha, J., Wan, DC (2011). "Numerical simulation of wave run-up around a vertical cylinder," *Proc 21st International Offshore and*

*Polar Engineering Conference*, b: 726-733.

Carrica, P.M., Wilson, R.V., Noack, R.W., Stern, F (2007). "Ship motions using single-phase level set with dynamic overset grids," *Computers & Fluids*, 36(9): 1415-1433.

Hirt, C.W., Nichols, B.D (1981). "Volume of fluid (VOF) method for the dynamics of free boundaries," *Journal of Computational Physics*, 39(1): 201-225.

Noack, R.W (2005). "SUGGAR: a general capability for moving body overset grid assembly," *In the Proceedings of the 17th AIAA Computational Fluid Dynamics Conference*, Toronto, Ontario, Canada, AIAA 2005-5117.

OpenFOAM (2013). "Mesh generation with the snappyHexMesh utility," Available from: [http://www.openfoam.org/docs/user/snappyHexMesh.php#x2\\_6-1510005\\_4](http://www.openfoam.org/docs/user/snappyHexMesh.php#x2_6-1510005_4).

Silva, G.A.L.d., Arima, M.N., Sousa, F.D.d (2010). " Mesh Generation in OpenFoam® with SnappyHexMesh," Available from: [http://www.ats4i.com.br/en/publications/files/SnappyHexMesh\\_1stOpenFoamBRAZIL\\_linux.pdf](http://www.ats4i.com.br/en/publications/files/SnappyHexMesh_1stOpenFoamBRAZIL_linux.pdf).

Shen, Z., Cao, H., Ye, H., Liu, Y., Wan, DC (2013). "Development of CFD Solver for Ship and Ocean Engineering Flows," *In 8th International OpenFOAM Workshop*, Jeju, Korea.

Shen, Z and Wan, DC (2012). "Rans computations of added resistance and motions of ship in head waves," *in Proceedings of the Twenty-second International Offshore and Polar Engineering Conference*, Kitakyushu, Japan, ISOPE, 3, 1096-1103.

Shen, Z., Jiang, L., Miao, S., Wan, DC, Yang, C (2011). "RANS Simulations of Benchmark Ships Based on Open Source Code," *In Proceedings of the Seventh International Workshop on Ship Hydrodynamics*, Shanghai, China, 76-82.

Shen, Z., Wan, DC (2013). "RANS Computations of Added Resistance and Motions of a Ship in Head Waves," *International Journal of Offshore and Polar Engineering*, ISOPE, 23(4): 263-271.

Shen, Z., Wan, DC (2015). "Manual of naoeFoam-os-SJTU Solver", Technical Report No. 2015SR012974, Shanghai Jiao Tong University.